6ᵗʰ International Symposium on Highway Capacity and Quality of Service
Stockholm, Sweden June 28 – July 1, 2011

Traffic Flow Characteristics and Capacity in Police-enforced and Intelligent Work Zones

Kivanc A. Avrenli [a],*, Rahim Benekohal[b], Hani Ramezani[a]

[a]Research Assistant, Department of Civil and Environmental Engineering, University of Illinois, Urbana Champaign,USA
[b]Professor, Department of Civil and Environmental Engineering, University of Illinois, Urbana Champaign,USA

Abstract

The effects of police enforcement on vehicle speeds in freeway work zones were examined in several studies. Likewise, many past studies investigated the effects of ITS implementation on vehicle speeds in freeway work zones. However, the effects of police enforcement and ITS implementation on work zone traffic flow characteristics and capacity have not yet been extensively studied. Hence, this study investigates the distinct effects of police enforcement and ITS implementation on work zone speed-flow curve and capacity. Three sets of traffic data were collected in a two-lane-open work zone located on I-55 near Chicago. The first data set was collected when there was only the traditional Manual of Uniform Traffic Control Devices (MUTCD) signage in the work zone. The second and the third data sets were collected when there was additionally police enforcement and Speed Photo Enforcement (SPE) in the work zone, respectively.
  The results showed that both the police enforcement and SPE led to significant changes in the work zone speed-flow curve compared to only MUTCD signage conditions. The general shape of the speed-flow relationship inside the work zone was similar to the speed-flow curve under basic freeway conditions, but the bending point of the upper branch of the curve occurred at lower traffic flow rates and the rate of the decrease in speed was higher. The speed-flow curve for the MUTCD signage-only case returned a work zone capacity of around 1,850 passenger cars per hour per lane (pcphpl). Compared to that speed-flow curve, both the police enforcement and SPE moved the upper (uncongested) branch of the speed-flow curve downward, which caused a work zone capacity reduction of about 50 pcphpl in the case of police enforcement and 100 pcphpl in the case of SPE implementation.
The results obtained through this study reveals the distinct effects of police enforcement and ITS on work zone capacity. Accurately estimating the capacity of work zones with different speed reduction treatments provides more efficient operation in a real-time system, more accurate diversion and traveler information for alternate routing, improved reliability of the system, and better understanding of the traffic flow characteristics in work zones.
© 2011 Published by Elsevier Ltd. Open access under CC BY-NC-ND license.

Keywords: Work zone capacity; police enforcement; speed photo enforcement; intelligent transportation systems; speed flow curve

* Corresponding author. Tel.: +1-217-819-9316.
  E-mail address: avrenli2@illinois.edu.

1. Introduction

Highway work zones continue to be a safety concern in the US. In 2007, motor vehicle crashes in U.S. work zones led to 835 fatalities and 105 fatal occupational injuries (National Work Zone Safety Information Clearinghouse, 2008). In terms of billion dollars spent, the highway work zone fatalities amount to at least four times more than the total U.S. construction (Mohan & Gautam, 2002). Thus, the crash data for U.S. highway work zones already indicate alarming rates.

According to Garber and Zhao (2002), rear-end collisions are the most predominant type of crashes in work zones, accounting for 83 percent of the total crashes in the advance warning areas of the highway work zones in Virginia. Salem, Genaidy and Deshpande (2006) and Garber and Zhao (2002) state that the predominance of rear-end collisions in highway work zones is attributed to high speed variation among vehicles and excessive vehicle speeds. Therefore, speed control strategies in work zones such as police enforcement and ITS implementation is primarily targeted at preventing the speeding of drivers to minimize speed variation. Several past studies investigated the efficacy of police enforcement and ITS on speed reduction in work zones. However, the effects of police enforcement and ITS on work zone capacity have not been extensively investigated. Considering this, the objectives of this study are as follows:

- How does the work zone speed-flow relationship change when there is either police enforcement or ITS implementation?
- How does the work zone capacity change when there is either police enforcement or ITS implementation?

2. Literature review

The speed-reduction effects of police enforcement and ITS in work zones were investigated several times. Nevertheless, their effects on work zone capacity were not extensively analyzed. Noel, Dudek, Pendleton and Sabra (1988) investigated the speed-reduction effects of implementing a marked police car with the light bar and radar active in a work zone where the speed limit was 45 mph. According to the results of their study, the police presence led to mean speed reductions of around 3.5 – 4.0 mph in the work zone. Zech, Mohan and Dmochowski (2005) evaluated the additional speed-reduction effects of police presence when it was utilized in combination with rumble strips in work zones. While the rumble strips alone could reduce the mean speed of merging vehicles by 1.4 – 2.9 mph, the police presence combined with rumble strips not only reduced by mean speeds by 4.0 – 6.0 mph, but also reduced the standard deviation of all vehicle speeds by about 25%. Most recently, Miller, Lindsay, Mannering and Abraham (2009) analyzed the effectiveness of various speed-control strategies in nighttime work zones in Indiana. According to the results of their study, indicator of police presence reduced the mean speed by 5.3 mph in the work zone. Miller, Lindsay, Mannering and Abraham (2009) also observed the speed-reduction effects of changeable message signs (a type of ITS) in nighttime work zones in Indiana, but the speed reductions induced by the changeable message signs turned out to be statistically insignificant. Nevertheless, none of the aforementioned studies investigated the effects of police enforcement on work zone capacity.

There is limited number of past studies that examined the effects of ITS on work zone capacity. Kang, Chang and Zou (2004) proposed a variable speed limit system that involved speed sensors, variable speed limit signs, changeable message signs and a central processing unit to carry out the control actions. By utilizing CORSIM simulations, they found that the variable speed limit system could increase the work zone throughput by up to 20 percent and reduce the average delay per vehicle by up to 34 percent. Next, Kang, Chang and Panacha (2006) explored the efficacy of dynamic late merge control in a work zone located on US Route I-83 in Maryland. They collected traffic data both under no-merge control and under dynamic late merge control. Using the same input traffic volumes and traffic compositions that had been observed in the field under the late-merge control, they simulated the traffic conditions under no merge control. Comparison of the simulation results and the results from the field data showed that the dynamic late merge led to up to 11 percent increase in work zone throughput compared to no-merge control.

Moreover, Yulong and Leilei (2007) developed an intelligent lane merge control system similar to dynamic late merge. Their system also utilized intelligent traffic information detection methods to choose the best merge control strategy, but is a combinative use of dynamic late merge with dynamic early merge instead of with the conventional merge control. They compared the effectiveness of static late merge control, dynamic early merge control, dynamic

late merge control and intelligent lane merge control strategies by using VISSIM simulations. According to the results, dynamic late merge control and intelligent lane merge increased the work zone capacity by eight and 20 percent, respectively, compared to the static late merge control.

3. Data collection and reduction

This objective of this study is to observe the distinct effects of police enforcement and ITS implementation on work zone speed-flow relationship and capacity. In order to capture the distinct effects of police enforcement and ITS deployment, three data sets were collected in a work zone located on I-55 NB at mile post 259. There were two lanes open to traffic in the work zone and it did not have any lane closure. The activity area was separated from the open lanes through concrete barriers. The work activity in the work zone was lane addition and bridge deck repair and the posted speed limit in the work zone was 55 mph (88.5 kph). All three data sets were collected during the off-peak hours in the afternoon in June, 2007. In order to avoid the effects of volume variation, all three data sets were collected during weekdays and at similar times of day. Moreover, no data collection was carried out during the peak traffic periods since high traffic volumes could have obscured the speed-reduction effects of the treatments. The traffic flow data were collected in the work zone for the following three scenarios:

1- Base data: There was no speed reduction treatment conducted in the work zone other than the traditional MUTCD signage.

2- Police data: A visible police patrol car and a police officer were present in the work zone in addition to the traditional MUTCD signage.

3- SPE data: An SPE van was implemented in the work zone as a speed control measure besides the traditional MUTCD signage.

Each data set involves approximately one hour of traffic flow data. In order to obtain information on individual vehicles, the traffic flow data were collected by a video camera. The video camera was situated such that it did not interfere with the work zone traffic flow. The research team placed two markers around 200 ft (61 m) apart from each other near the shoulder. Vehicles passing the two markers were captured by the video camera. The markers were situated several hundred feet downstream of the treatment location, (i.e. either the police car or the SPE van), so that the motorists had sufficient space to respond to the treatment by reducing their speeds before they were captured by the video camera. The research team also recorded some general information about the work zone layout, weather conditions and the position of ramps in close proximity. All vehicles that made lane change between the two markers were excluded from the data. In each data set, the number of vehicles that made lane change between the two markers was less than 0.5 percent of the total number of vehicles observed.

Time stamps and frame numbers in the video files provided accurate reading of a particular frame within 1/30th of a second. The following data were obtained for each vehicle from the video files in all three data sets:

1. Vehicle type classified into two categories as follows:
   i. Passenger cars (PC): Cars, pickup trucks, sport utility vehicles and minivans.
   ii. Heavy vehicles (HV): Single-unit trucks, semitrailers, combination trucks and buses.
2. Lane of travel:
   i. Median lane
   ii. Shoulder lane
3. Times at which the vehicle passed the two markers.

In order to compute the speed of a particular vehicle, the time at which it passed the two markers were used. Moreover, by using the times at which successive vehicles passed one of the selected markers, vehicle headways were computed.

4. Analysis and results

4.1. Work zone speed-flow curve for the base data

The work zone speed-flow curve for the Base data comes from the study by Avrenli, Benekohal and Ramezani (2011). The upper (uncongested) branch of the work zone speed flow curve was obtained from the Base data as a two-regime model. The first one is the free flow regime, which is a straight line at the free flow speed of 59.1 mph (95 kph) between the range of zero and 800 pcphpl. The second one is the transition regime, where the average

speeds start decreasing with the increasing flow rate. For the Base data, the transition regime occurs between the flow rates of 800 and 1,900 pcphpl where 1,900 pcphpl is the estimated capacity of the work zone.

On the other hand, the lower branch of the speed-flow curve consists of the congestion regime. Since no congestion was observed at that site during the data collection period, the congestion data were obtained from two single-lane work zones, one on I-74 EB at mile post 5 and the other on I55 NB at mile post 55. It should be noted that those two work zones differed geometrically from the two-lane-open work zone on I55 NB, but the authors believe that the congestion data could give a similar illustration for the congested flow conditions in the two-lane-open work zone on I-55 NB. The free flow, transition and congestion regimes of the work zone speed-flow curve for the Base scenario are represented by Equations (1), (2) and (3), respectively.
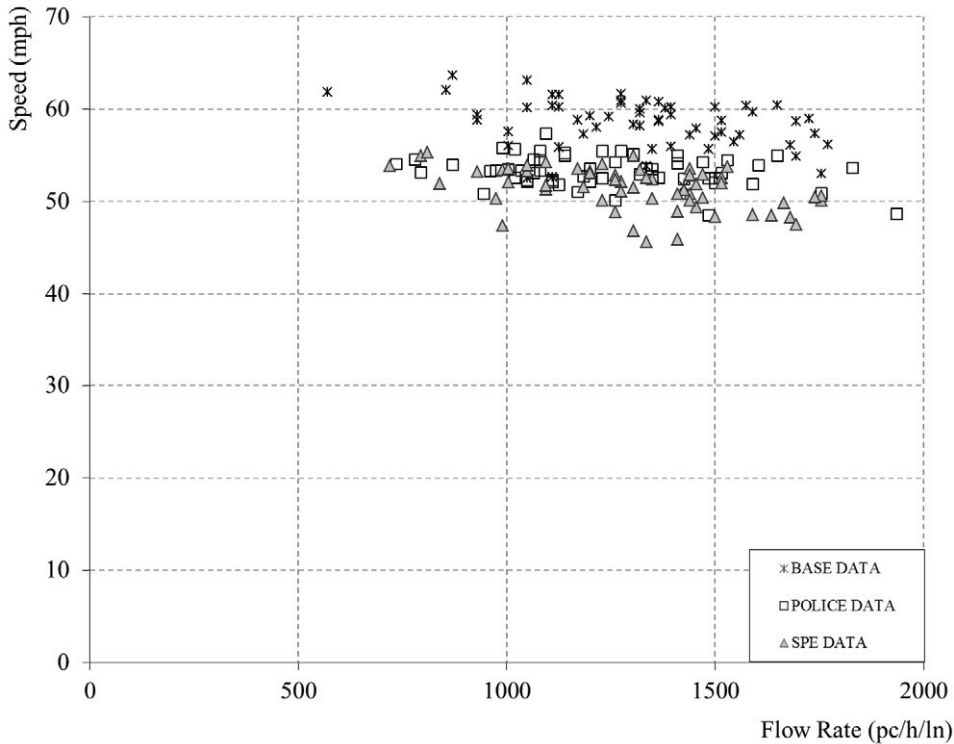

Figure 1 Scatterplot of the Base, Police and SPE data

$$U = FFS \tag{1}$$

$$U = FFS - (FFS - 20.6) * \left(\frac{Q-800}{2208-22.9*FFS}\right)^{3.6} \tag{2}$$

$$Q = 271.43 * U^{0.4868} \tag{3}$$

where
    U = Average speed (mph),
    FFS = Free flow speed (found as 59.1 mph by nonlinear regression for the Base data),
    Q = Flow rate (pcphpl).

4.2. Work zone speed-flow curves for the police and SPE data

In this section, first, the Police and SPE data are compared with the Base data. Then the upper (uncongested) branches of the speed-flow curves are set as two-regime models: Free-flow regime and transition regime. As for the lower (congested) branch of the speed-flow curves, the same congestion model as suggested by Avrenli, Benekohal

and Ramezani (2011) is used to represent the congested traffic conditions in the work zone. Finally, the three-regime speed flow curves are fine-tuned as four-regime models to more realistically represent the speed-flow relationship in close-to-capacity conditions.

4.2.1. Comparing the base data with the police and SPE data

The mean speeds and mean flow rates are summarized for each data set in Table 1. Unpaired t-tests were conducted to make pairwise comparisons of the mean flow rates and mean speeds among the Base, Police and SPE data. According to the results of the t-tests, it was found that the mean speeds changed in the following order at $\alpha=0.05$: Base > Police > SPE. On the other hand, it was found from the t-tests that the mean flow rates of the three data sets did not differ significantly from each other at $\alpha=0.05$. Since all other factors such as weather conditions, lane width and work intensity were the same for all three data sets during the data collection, the significant speed reductions for the Police and SPE data are attributed to the presence of the police car and SPE van in the work zone, respectively.

Table 1 The mean and standard deviation of the speed and flow rate for each data set

Data set	Mean speed (mph)	Standard deviation of speed (mph)	Mean flow rate (pcphpl)	Standard deviation of flow rate (pcphpl)
Base	58.4	2.6	1321	257
Police	53.1	2.0	1239	259
SPE	51.4	2.3	1301	253

4.2.2. Free-flow regime

For both the Police and SPE data, the scatter plots of the speed-flow data indicate that the speed-flow relationship tends to level up as the flow rate decreases towards 800 pcphpl. Thus, it is also assumed for both the Police and SPE data that free flow takes place up to a flow rate of 800 pcphpl. However, Figure 1 shows that very few data points exist below the flow rate of 800 pcphpl for the data sets. Thus, the free-flowing vehicles were analyzed separately to better estimate the free-flow regime of the speed-flow curves. In this study, it is assumed that a vehicle undergoes free-flow conditions if its time headway is greater than 4.0 s and if its space headway is greater than 250 ft (76 m). Figure 2a and 2b shows the scatterplot of speed vs. headway for the free-flowing vehicles for the Police and SPE data. Neither Figure 2a nor 2b exhibits any trend between headway and speed. In other words, there is no obvious increase in speed as the headways increases and the instantaneous flow rate decreases. Thus, it is assumed for both data sets that the free-flow regime is a horizontal line between the flow rates of zero and 800 pcphpl.
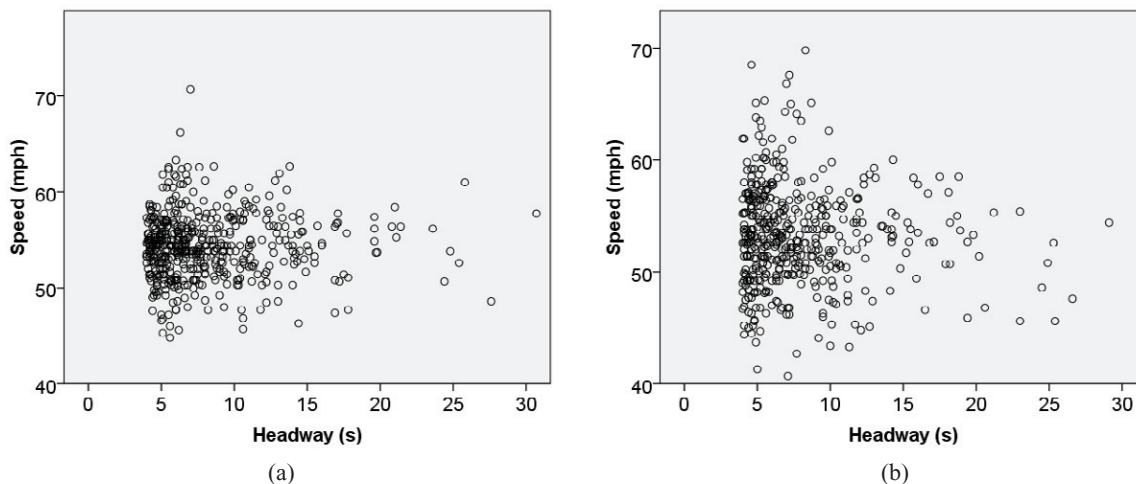

Figure 2 Scatterplot of speed vs. headway of the free-flowing vehicles for the (a) Police data, (b) SPE data.

4.2.3. Transition regime

For both the Police and SPE data, the transition regime for the work zone corresponds to the flow range between 800 pcphpl and Q_{max} where Q_{max} represents the work zone capacity. To represent the speed-flow relationship in the transition regime, a nonlinear regression model in the form of Equation is fit to the scatterplots in Figure 1. The format of Equation (2) is similar to that suggested by HCM 2000 for basic freeway sections. Nonetheless, it is set based on the assumption that free flow takes place as the flow rate falls below 800 pcphpl. Nonlinear regression was carried out to determine the parameters in Equation (2). The nonlinear least squares estimation returned the coefficients given in Equations (4) and (5) for the Police and SPE data, respectively:

$$U = FFS - (1.0 * FFS - 22.7) * \left(\frac{Q - 800}{2242 - 3.3 * FFS} \right)^{3.6} \tag{4}$$

$$U = FFS - (1.1 * FFS - 15.9) * \left(\frac{Q - 800}{2143 - 4.9 * FFS} \right)^{3.6} \tag{5}$$

where

FFS = Free flow speed found as 53.6 mph (86.2 kph) and 52.1 mph (83.8 kph) from the nonlinear regression for the Police and SPE data, respectively.

U = Average speed (mph); $U_{optimum} < U < FFS$ where $U_{optimum}$ is the speed at the maximum flow rate.

Q = Flow rate (pcphpl); $800 \leq Q \leq Q_{max}$.

Hence, Equation (4) and (5) represent the work zone speed-flow relationship for the Police and SPE data, respectively, when neither free flow nor flow break-down occurs. Since the free flow speed is estimated as 53.6 mph and 52.1 mph for the Police and SPE data, respectively, from the nonlinear regression analysis, the free flow regime is set as a horizontal line at 53.6 mph and 52.1 mph between the flow rates of zero and 800 pcphpl for the Police and SPE data, respectively. The lower bound of the transition regime is 800 pcphpl whereas the upper bound is to be determined for each data set after the congestion regime is set. The free-flow and the transition regimes are plotted along with the scatterplot of the data in Figure 3.
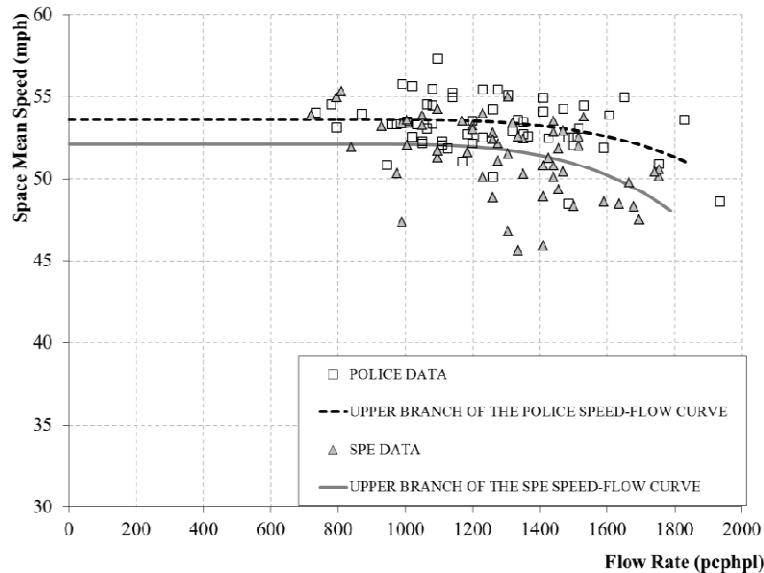

Figure 3 Upper branches of the speed-flow curves for the Police and SPE data

4.2.4. Congestion regime

The authors believe that the speed-flow relationship in congested traffic would not differ appreciably with regard to the type of traffic enforcement in the work zone. Thus, it is assumed that the speed-flow relationship for congested traffic is the same for the Base, Police and SPE data. Hence, the power function in Equation (3) is assumed to represent the speed-flow relationship in congested traffic for both the Police and SPE data. Figure 4

indicates the completed three-regime speed-flow curves for the police and SPE data.
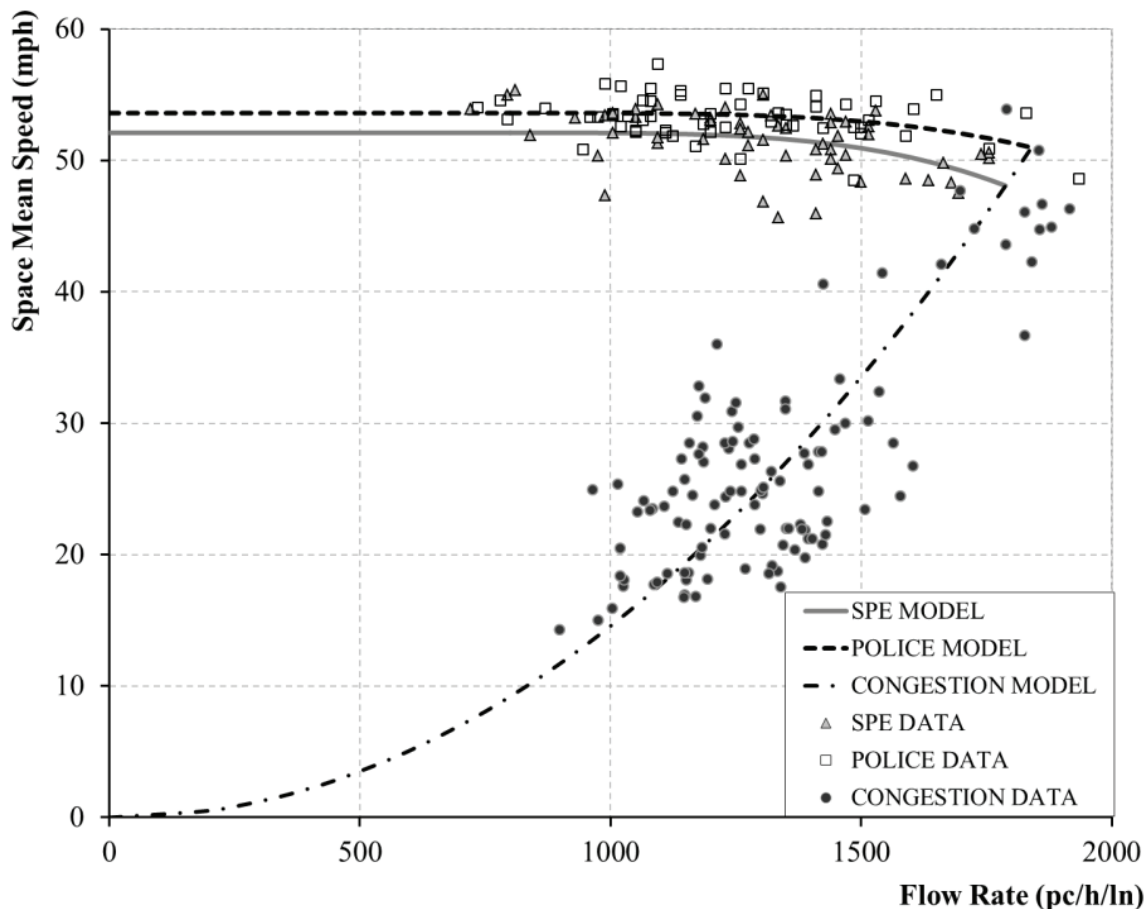

Figure 4 Completed three-regime speed-flow curves for the Police and SPE data

4.3. Fine-tuning the speed-flow curves

Avrenli, Benekohal and Ramezani (2011) recommended the improvement of three-regime speed-flow curves to avoid sharp transition between the congested (lower) and uncongested (upper) branches. The speed-flow curves in Figure 4 may not accurately depict the speed-flow relationship in the field close to capacity conditions due to the sharp transition from the uncongested regime to the congested regime. Thus, the final speed-flow curves need to be fine-tuned. In this section, the speed-flow curves are improved to four-regime models to smoothen the transition between the upper and lower branches of the speed flow curves.

Figure 5 illustrates the general form of the four-regime speed-flow curves. The four-regime models differ from the three-regime models in that they have upper and lower transition regimes instead of a single transition regime. The free-flow and upper transition regimes represent the traffic conditions with no flow break-down. On the contrary, the lower transition and congestion regimes represent the traffic conditions when flow break-down occurs. As shown in Figure 5, the upper transition regime is the part of the speed-flow curve between the end of the free-flow regime and the point of maximum flow. On the other hand, the lower transition regime connects the upper transition regime to the congestion regime, providing a smooth transition at the point of maximum flow.
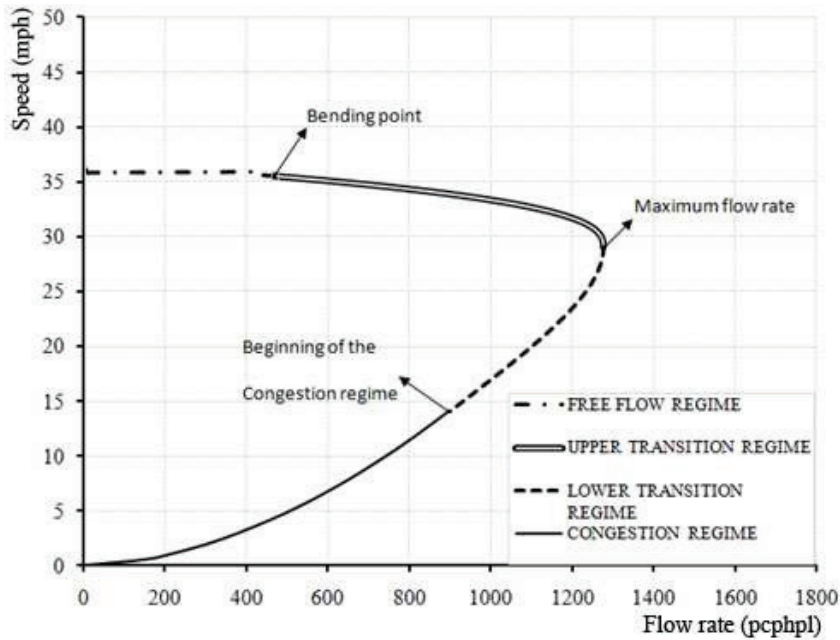
Figure 5 General form of the four-regime speed-flow curve

Polynomial functions of degree four were used for the upper regimes. Equation (6) shows the general form of these functions:.

$$Q = A * U^4 + B * U^3 + C * U^2 + D * U + E \qquad\qquad (6)$$

where
    Q = Flow rate (pcphpl).
    U = Speed (mph).
    A, B, C, D, E = The coefficients of the polynomial function.

According to Figure 5, the domain of each regime is set by determining three points, namely the bending point, the point with the maximum flow rate and the beginning of the congestion regime. These points are determined as below:

- The free-flow regime is a horizontal line for all speed-flow curves. The bending point is the end of the free flow regime and the beginning of the upper transition regime. In this study, all the bending points have a flow rate of 800 pcphpl as it is assumed that free flow takes place at flow rates less than 800 pcphpl. For each speed-flow curve, the free-flow speed is the average speed of the free-flowing vehicles (excluding the platoon leaders). The free-flow speeds are 61.3 mph (98.6 kph), 55.0 mph (88.5 kph), and 54.5 mph (87.7 kph) for the Base, Police and SPE data, respectively.
- The upper transition and lower transition regimes are connected at the point with the maximum flow rate and optimum speed. For the Base, Police and SPE data, the points with the maximum flow rate are determined by using the same methodology proposed by Ramezani, Benekohal and Avrenli (2011). The results are summarized in Table 2. The second column of Table 2 gives the maximum flow rate computed from the "h-n method" suggested by Ramezani, Benekohal and Avrenli (2011). The third column of Table 2 gives maximum flow rate computed from the average headway of in-platoon vehicles during the peak 15-minute. The fourth column shows the "platooning factor" computed by dividing column two by the 95 percent of column three. The work zone capacity is estimated by multiplying column three by the corresponding platooning factor in column four. The sixth column gives the estimated work zone capacity rounded to the nearest 50 pcphpl. To compute the optimum speed, the speed corresponding to the flow rate in column six of Table 2 is found from Equations (2), (4) and (5) for the Base, Police, and SPE data, respectively. Then for each data set, that speed is reduced by 1.0 mph and

taken as the optimum speed. Column seven of Table 2 gives the optimum speed for each data set. It should be noted that the results given in Table 2 are the average results for the median and shoulder lanes for each data set.

Table 2 Summary of the work zone capacity calculations

Data set	Max. flow rate from the "h-n method" (C_1) (pcphpl)	Max. flow rate from the platooning vehicles (C_p) (pcphpl)	Platooning factor (PF) $\left(\dfrac{C_1}{C_p + 0.95}\right)$	Work zone capacity (PF*C_p)	Work zone capacity rounded to the nearest 50 (pcphpl)	Speed at capacity (mph)
BASE	1748	2392	0.77	1840	**1850**	**54.2**
POLICE	1689	2453	0.72	1777	**1800**	**50.3**
SPE	1665	2362	0.74	1753	**1750**	**47.6**

- The flow rate at the beginning of the congestion regime is assumed to be 1300 pcphpl for all speed-flow curves. This flow rate is chosen to maintain the overall shape of the lower branch of the speed-flow curves as close as possible to Equation (3) since Equation (3) was constructed based on the field data.
- The congestion regime for each speed-flow curve is the same as Equation (3).

The coefficients of the upper transition model in Equation (6) are determined by fitting a cubic spline between the bending point and the point with maximum flow rate. Likewise, the coefficients of the lower transition model in Equation (6) are determined by fitting a cubic spline between the point with the maximum flow rate and beginning of the congestion regime. Given the points at which two adjacent regimes connect to each other, the coefficients were calculated such that the functions of the two adjacent regimes had equal value, equal first derivative and equal second derivative at the connection point. In addition, the first derivative of the upper and lower transition regimes was set to zero at the point with the maximum flow rate. The equations of the upper transition and lower transition models are given in Table 3 for each data set. Moreover, Figure 6 shows the four-regime speed-flow curves on a single chart, revealing the effects of the police car and SPE van on the speed-flow relationship. Because both the police car and SPE van led to significant reductions in speed in the upper branch of the speed-flow curve, the work zone capacity was slightly reduced in both cases compared to the Base data.
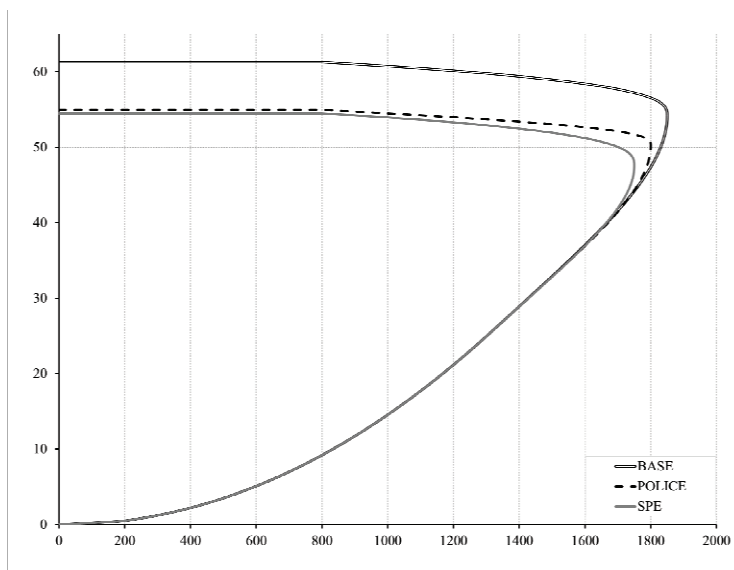

Figure 6 Four-regime speed-flow curves for the Base, Police and SPE data

Table 3 Equations for the upper transition and lower transition regimes for each data set

Data set	Upper transition equation	Lower transition equation
Base	$Q = 0.097 * U^4 - 24.5 * U^3 + 2,268 * U^2 - 91,968 * U + 1,388,267$	$Q = -0.0002312 * U^4 + 0.0222 * U^3 - 0.799 * U^2 + 38.1 * U + 591$
Police	$Q = 2.219 * U^4 - 466.3 * U^3 + 36,664 * U^2 - 1,279,206 * U + 16,712,680$	$Q = -0.0005257 * U^4 + 0.0571 * U^3 - 2.311 * U^2 + 66.7 * U + 391$
SPE	$Q = -0.000489 * U^4 - 2.52 * U^3 + 364.3 * U^2 - 17,356 * U + 276,518$	$Q = -0.0007751 * U^4 + 0.0843 * U^3 - 3.416 * U^2 + 86.5 * U + 258$

5. Conclusions and recommendations

This study examined the distinct effects of police enforcement and ITS implementation on work zone speed-flow relationship and capacity. According to the results, both the police enforcement and the SPE van altered the speed-flow relationship by lowering the speeds in the upper (uncongested) part of the speed-flow curve. Because both the police car and SPE van reduced the speeds in the upper branch of the work zone speed-flow curve, a slight capacity reduction of around 50 pcphpl and 100 pcphpl was for the Police and SPE data, respectively.

Accurate estimation of work zone capacity enables more effective operation on a real-time basis, more accurate diversion and traveler information for alternate routing and enhanced system reliability. Besides, it brings about improved knowledge on the characteristics of traffic flow in work zones with various speed reduction treatments. In the meantime, the effects of other types of ITS on work zone operating speed and operating capacity have not yet been investigated. Therefore, it is recommended as future research that the effects of other types of ITS such as changeable message signs, variable speed limits and dynamic late merge in highway work zones be investigated. Thereby, a wider understanding of the traffic flow characteristics in intelligent work zones can be gained. It is also recommended to conduct the study for work zones with different speed limits and various lane configurations.

References

Avrenli, K. A., Benekohal, R., & Ramezani H. (2011) Determining the Sped-Flow Rleationship and Capacity for a Freeway Work Zone with no Lane Closure. *Presented at the 90th TRB Annual Meeting*, Washington, D.C., January, 2011.

Garber, N. J., & Zhao M. (2002) Distribution and characteristics of crashes at different work zone locations in Virginia. *Transportation Research Record, Journal of the Transportation Research Board*, 1794, 19 – 28.

Highway capacity manual (HCM). (2000). Transportation Research Board: National Research Council, Washington, D.C.

Kang, K., Chang, G., & Panacha J. (2006) Optimal dynamic speed-limit control for highway work zone operations. *Transportation Research Record: Journal of the Transportation Research Board*, 1948, 86 – 95.

Kang, K., Chang, G., & Zou N. (2004) Optimal dynamic speed-limit control for highway work zone operations. *Transportation Research Record: Journal of the Transportation Research Board*, 1877, 77 – 84.

Miller, L., Mannering, F., & Abraham D. M. (2009) Effectiveness of speed control measures on nighttime construction and maintenance projects. *Journal of Construction Engineering and Management*, 135 (7), 614 – 619.

Mohan, S. B., & Gautam P. (2002) Cost of highway work zone injuries. *Practice Periodical on Structural Design and Construction*, 7 (2), 68 – 73.

National Work Zone Safety Information Clearinghouse. (2008). *Fatalities in motor vehicle traffic crashes by state and construction/ maintenance zone (2007)*. Retrieved February 10, 2010 from http://www.workzonesafety.org/crash_data/workzone_fatalities/2007.

Noel, E. C., Dudek, C. L., Pendleton, O. J., & Sabra Z. A. (1988) Speed control through freeway work zones: Techniques evaluation. *Transportation Research Record*, 1163, 31 – 42.

H. Ramezani, R. Benekohal, and K. Avrenli (2011). Methodology to Measure Work Zone Capacity Using Field Data. *Presented at the 90th TRB Annual Meeting*, Washington, D.C., January, 2011.

Salem, O.M., Genaidy, A. M., Wei, H., & Deshpande N. (2006) Spatial distribution and characteristics of accident crashes at work zones of Interstate Freeways in Ohio. *Proceedings of ITSC 2006: 2006 IEEE Intelligent Transportation Systems Conference,*1642 – 1647.

Yulong, P., & Leilei D. (2007) Study on intelligent lane merge control system for freeway work zones. *Proceedings, ITSC, 10th International IEEE Conference on Intelligent Transportation Systems*, 586 – 591.

Zech, W. C., Mohan, S., & Dmochowski J. (2005) Evaluation of rumble strips and police presence as speed control measures in highway work zones, *Practice Periodical on Structural Design and Construction*, 10 (4), 267 – 275.